Damascus University Journal of Earthquake and DisasterResearch مجلة جامعة دمشق وبحوث الزلازل الكوارث
Vo 3 number (1) -2026: 61-78 المجلد 3 العدد (1) – 2026: 61-78

Analytical study of seismic response of existing RC bridges with a variable damping ratio

Mais Adeeb Ghassoun*[1] Reem Salman ALsehnawi[2]

*[1]. Dr, lecturer, Faculty of Engineering, Wadi International University – Homs – Syria.
dr-maisghassoun@wiu.edu.sy

[2]. Dr, lecturer, Higher Institute of Earthquake Studies and Researches, Damascus University– Damascus –Syria.
reem1.salman@damascusuniversity.edu.sy

Received: 4/3 /2026
Accepted: 13/4/2026

Abstract:

The seismic response of structures is influenced by variations in dynamic properties, which change with vibration amplitude. In this study, two analytical models simulating experimental single-span RC bridges were developed using ABAQUS software. The connection between the slab and the pier was modeled as fixed in one case and as lead rubber bearings (LRB) in the other.Considering the equation proposed by Ghassoun et al. (2023), which describes the relationship between damping ratio and acceleration amplitude, the seismic responses of the analytical and experimental models were compared to verify the validity of this formulation. Subsequently, the proposed equation was applied to an existing RC bridge in Homs city, consisting of two spans and three piers, to investigate the influence of damping ratio variation on seismic response. The lateral displacements, accelerations, and shear forces were evaluated and compared for both constant and variable damping ratios. The results demonstrated that the numerical and analytical responses obtained using the variable damping model are in good agreement with the experimental results, with differences in the range of 1.5–2.2%, compared to 38–58% for the constant damping assumption. Furthermore, the variable damping ratio resulted in higher estimated seismic responses than the constant damping case.

Key words: Seismic analysis, Existing RC Bridge, Seismic response, damping ratio variation, acceleration amplitude.

http://journal.damascusuniversity.edu.sy/index.php/index/index
X085-3031 :ISSN (online)

دراسة تحليلية للاستجابة الزلزالية للجسور الخرسانية المسلحة القائمة مع اعتبار نسبة التخميد المتغيرة

ميس أديب غصون*[1] ريم سلمان الصحناوي[2]

*[1]. دكتورة، مدرّسة في كليّة الهندسة– جامعة الوادي الدولية الخاصّة – حمص – سوريا.
dr-maisghassoun@wiu.edu.sy

[2]. مدرّسة في المعهد العالي للبحوث و الدراسات الزلزاليّة– جامعة دمشق- دمشق - سوريا.
reem1.salman@damascusuniversity.edu.sy

تاريخ الايداع: 2026/3/4
تاريخ القبول: 2026/4/13

الملخص:

يتأثر السلوك الزلزالي للمنشآت بالتغيرات في خصائصها الديناميكية، والتي تتبدل مع تغيّر سعة الاهتزاز. في هذه الدراسة، تم تطوير نموذجين تحليليين لمحاكاة جسور خرسانية مسلحة أحادية الفتحة تم اختبارها تجريبياً، وذلك باستخدام برنامج ABAQUS. وقد تم تمثيل الوصلة بين البلاطة والركيزة على أنها تثبيت تام في الحالة الأولى، بينما استُخدمت محامل مطاطية رصاصية (LRB) في الحالة الثانية. وبالاعتماد على المعادلة المقترحة من قبل Ghassoun et al. (2023)، والتي تصف العلاقة بين نسبة التخميد وسعة التسارع، تمت مقارنة الاستجابات الزلزالية للنماذج التحليلية والتجريبية للتحقق من صحة هذه الصيغة. بعد ذلك، تم تطبيق المعادلة المقترحة على جسر قائم فيHoms ، يتكون من فتحتين وثلاث ركائز، وذلك لدراسة تأثير تغير نسبة التخميد على الاستجابة الزلزالية. تم تقييم ومقارنة الإزاحات الجانبية والتسارعات وقوى القص لكل من حالتي التخميد الثابت والمتغير. وأظهرت النتائج أن الاستجابات العددية والتحليلية الناتجة باستخدام نموذج التخميد المتغير تتوافق بشكل جيد مع النتائج التجريبية، حيث تراوحت الفروقات بين 1.5% و2.2%، مقارنةً بفروقات تتراوح بين 38% و58% عند افتراض التخميد الثابت. علاوة على ذلك، أدى استخدام نسبة التخميد المتغيرة إلى تقدير استجابات زلزالية أعلى مقارنةً بحالة التخميد الثابت.

الكلمات المفتاحية: تحليل زلزالي، جسر بيتوني قائم، استجابة زلزالية، تغيرات نسبة التخامد، سعة التسارع.

Introduction:

The relationship between dynamic properties and seismic response of reinforced concrete (RC) bridges is critical to ensuring structural integrity during seismic events. Dynamic properties, such as natural frequencies and mode shapes, have a significant influence on how bridges respond to seismic loads.

Studies indicate that seismic responses are significantly higher than those under gravity loads, emphasizing the need for dynamic load considerations in bridge design [1].

The seismic analysis of existing reinforced concrete (RC) bridges requires an understanding of their response to seismic events, with particular emphasis on the effects of variations in damping ratio and acceleration amplitude.

The nonlinear seismic performance of RC bridges can be assessed using various methods, such as elastic (ESA), dynamic (EDA), and direct displacement-based assessment (DDBA), with nonlinear history analysis (NLTHA) providing a more accurate representation of inelastic responses, especially when considering different viscous damping models [2].

Finite element analysis, including response spectrum and time history analysis, is critical for evaluating seismic response and the effectiveness of retrofit methods such as restraints, which can improve dynamic properties such as displacement and base shear [3].

Non-linear dynamic analysis highlights the importance of passive control strategies, such as metallic dampers, which can significantly reduce horizontal displacements and maintain structural integrity under extreme seismic actions [4]. The accuracy of seismic response predictions is sensitive to the modelling of nonlinear load–deformation relationships, and methods such as those outlined in FEMA 273 and ATC-40 provide a framework for such analyses, although improvements in accuracy are still needed [5].

In addition, the choice of damping models, such as Rayleigh and Caughey formulations, can significantly influence seismic response predictions, as each model has specific applicability and limitations that must be carefully considered [6].

The high viscous damping coefficient can lead to structural damage during strong earthquakes, indicating a complex relationship between damping ratios and acceleration amplitudes [7].

Relying on experimental methods to investigate seismic behavior remains challenging due to the scale and energy requirements involved [8].

Other studies have related dynamic amplification factors to bridge characteristics such as natural frequency, mass, and structural configuration [9], while additional research has examined radiation damping effects and their dependence on geometric properties [10]. Furthermore, simplified and nonlinear numerical approaches, including Zeus NL software, have been employed to simulate seismic response of RC bridges under various assumptions [11].

Despite these advances, most existing seismic analysis and design approaches still rely on constant damping ratio assumptions, which may not adequately represent the actual energy dissipation mechanisms under varying excitation amplitudes. Recent studies have emphasized that damping properties in reinforced concrete structures are amplitude-dependent and evolve during seismic loading, which can significantly affect the accuracy of predicted structural responses [12–14].

Therefore, it is necessary to account for the variation of damping ratio with acceleration amplitude in order to achieve more realistic seismic response predictions. In this context, the present study aims to verify that dynamic responses obtained by considering variable damping ratio are more consistent with actual behavior than those assuming constant damping. This is achieved by integrating an acceleration-dependent damping formulation into both analytical and numerical models and validating the results against experimental data.

1-Research objective and methodology:

1.1 Research objective:

It is common practice to consider the damping ratio as a constant value in structural design; however, previous studies and experimental observations have shown that this assumption may be inaccurate, as the damping ratio varies with changes in excitation amplitude. Therefore, this study aims to investigate the effect of damping ratio variation on the seismic response of an existing RC bridge, after first verifying the validity of the acceleration amplitude–damping ratio relationship proposed by Ghassoun et al. (2023) [15].

1.2 Research methodology:

The adopted research methodology consists of three main stages, combining analytical modelling, numerical simulation, and experimental validation.

1- A numerical model was developed using Excel sheets for two experimental bridge models with fixed and lead rubber bearing (LRB) connections, based on a previous study. The general equation of motion was solved using initial conditions simulating the experimental setup, incorporating the variable damping ratio equation proposed by Ghassoun et al. (2023) [15].

2- Finite element models of the experimental RC bridges were constructed using ABAQUS software, considering a time-dependent damping ratio. The models were analyzed and validated by comparing the numerical results with the experimental responses in terms of free vibration behavior.

3- After validating the proposed equation, an existing RC bridge was modeled in ABAQUS using both constant and variable damping ratios to investigate the influence of damping variation on seismic response under the Turkey–Syria (Hatay) earthquake record (TK 3123 station).

2- Numerical study:

1-2 Models' description:

The geometrical and material properties of the experimental bridge models are summarized as follows:

The two models represent identical single-span RC bridges; however, the slab–pier connection was modeled as fixed in the first model and as lead rubber bearing (LRB) in the second model, as shown in Fig. 1.

The bridge slab has a rectangular cross-section of 150 × 400 mm and a length of 2200 mm, reinforced with 4T10 mm longitudinal bars and stirrups of 6 mm diameter spaced at 150 mm.

Each pier has a rectangular cross-section of 88 × 400 mm with a net height of 1500 mm, supported on a square base of 600 × 600 × 300 mm. The longitudinal reinforcement of each pier consists of 4T10 mm bars, with 6 mm stirrups spaced at 150 mm within the top and bottom 600 mm regions, and at 250 mm spacing in the central region.

The yield strength of the longitudinal reinforcement is 401 MPa, with a Young's modulus of 210 GPa. The unit weight of concrete is 23.4 kN/m³. The slab and pier were cast at different times; therefore, their material properties differ. The compressive strength of the slab is 52.2 MPa, with a Young's modulus of 26 GPa.

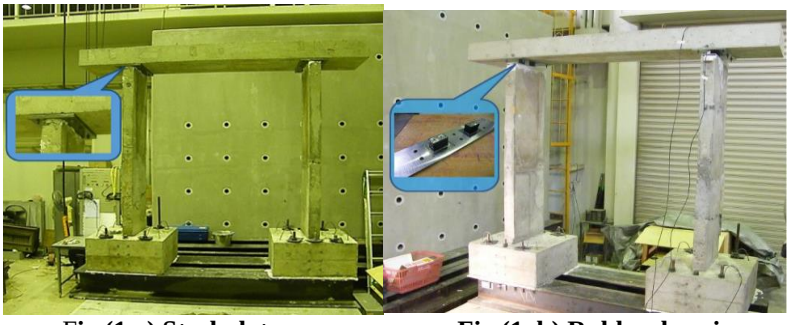

Fig (1.a) Steel plate **Fig (1. b) Rubber bearing**

Fig (1) Experimental RC Bridge Model [16]

2-2 Numerical analysis:

An analytical model was developed to represent the bridge elements using the coordinates of their end nodes, allowing the calculation of both stiffness and mass matrices. These were then assembled within the assumed general coordinate system (a vertical plane passing through the bridge elements), followed by static condensation of the effective degrees of freedom (Ld matrix).

The stiffness and mass corresponding to the first mode of free horizontal vibration were obtained at the two nodes connecting the piers to the slab. The mass of the protruding part of the slab was considered as a concentrated mass at these nodes. To determine the dynamic characteristics, the general equation of motion was solved assuming a single-degree-of-freedom system using Excel sheets at this stage.

The boundary conditions were defined by assuming an initial velocity at time t = 0 ($y = 0$, $y' = y'_0$, $y'' = 0$). The time step (Δt) was introduced for the numerical solution. The selection of the time step (Δt) was governed by the requirement to accurately capture the evolution of the damping ratio at each time instant of the applied seismic excitation. Since the adopted damping model is expressed as a function of the instantaneous acceleration amplitude, the time discretization must be fully consistent with the temporal resolution of the input ground motion record.

Accordingly, the adopted time step was taken equal to the sampling interval of the earthquake acceleration record, ensuring that the damping ratio is evaluated and updated at each recorded time point. This guarantees proper synchronization between the seismic input and the computed structural response, thereby enhancing the accuracy of the numerical simulation.

Based on the Duhamel integral and the derivation of the response quantities, the acceleration response was calculated and compared with the maximum experimental acceleration (Y''_{exp}) for each case. The calculation was performed iteratively by adjusting the assumed initial velocity until the computed acceleration satisfied $Y''_{n+1} \approx Y''_{exp}$. The corresponding initial velocity was then adopted.

Assuming an initial damping ratio $\xi = \xi_0$, the response was subsequently calculated using Eqs. (1), (2), and (3).

$$Y_{n+1} = (Y_n * \cos(\omega * t_{n+1}) + (Y'_n + Y_n * \xi * \omega_0)/\omega * \sin(\omega * t_{n+1})) * e^{(-\xi * \omega 0 * t_{n+1})} \quad (1)$$

$$Y'_{n+1} = (-Y_n * \omega * \sin(\omega * t_{n+1}) + (Y'_n + Y_n * \xi * \omega_0)/\omega * \omega * \cos(\omega * t_{n+1})) * e^{(-\xi * \omega 0 * tn+1)} - \xi * \omega_0 * e^{(-\xi * \omega 0 * t_{n+1})} * (Y_n * \cos(\omega * t_{n+1}) + (Y'_n + Y_n * \xi * \omega_0)/\omega * \sin(\omega * t_{n+1})) \quad (2)$$

$$Y''_{n+1} = (-Y_n * \omega^2 * \cos(\omega * t_{n+1}) - (Y'_n + Y_n * \xi * \omega_0)/\omega * \omega^2 * \sin(\omega * t_{n+1})) * e^{(-\xi * \omega_0 * tn+1)} + (-Y_n * \omega * \sin(\omega * t_{n+1}) + (y'_n + Y_n * \xi * \omega_0)/\omega * \omega * \cos(\omega * t_{n+1})) * e^{(-\xi * \omega 0 * tn+1)} * (-\xi * \omega_0) - \xi * \omega_0 * e^{(-\xi * \omega 0 * tn+1)} * (-Y_n * \omega * \sin(\omega * t_{n+1}) + (Y'_n + y_n * \xi * \omega_0) * \cos(\omega * t_{n+1})) + \xi^2 * \omega_0^2 * e^{(-\xi * \omega_0 * t_{n+1})} * (Y_n * \cos(\omega * t_{n+1}) + (Y'_n + Y_n * \xi * \omega_0)/\omega * \sin(\omega * t_{n+1})) \quad (3)$$

Were:

Y_{n+1}: the displacement at time (n+1)
Y'_{n+1}: the velocity at time (n+1)
Y''_{n+1}: the acceleration at time (n+1)
ω: angular frequency
ω_0: natural angular frequency
ξ: damping ratio

The displacements response was calculated from the equation of motion using the finite difference method (central difference). Considering a constant acceleration at each step, the responses for the constant and variable damping ratio were calculated. The New mark integration method was used by substituting the Eqs (4) and (5) [17] in the equation of motion to calculate the displacement from Eq. (6).

$$Z'_{(t+dt)} = (2 * Z_{(t+dt)} - 2 * Z_{(t)} - Z'_{(t)} * dt)/dt \quad (4)$$

$$Z''_{(t+dt)} = (4 * Z_{(t+dt)} - 4 * Z_{(t)} - 4 * Z'_{(t)} * dt)/(dt^2) - Z''_{(t)} \quad (5)$$

$$m((4 * Z_{(t+dt)} - 4 * Z_{(t)} - 4 * Z'_{(t)} * dt)/(dt^2) - Z''_{(t)}) + c((2 * Z_{(t+dt)} - 2 * Z_{(t)} - Z'_{(t)} * dt)/dt) + k(Z_{(t+dt)}) = 0 \quad (6)$$

Were:

$Z_{(t)}$: the displacement at time (t) — $Z_{(t+dt)}$: the displacement at time (t+dt)

$Z'_{(t)}$: the velocity at time (t) — $Z'_{(t+dt)}$: the velocity at time (t+dt)

$Z''_{(t)}$: the acceleration at time (t) — $Z''_{(t+dt)}$: the acceleration at time (t+dt)

dt: time step — m: mass

c: The damping coefficient — K: stiffness

The damping ratio is compared with the eq (7):

$$f(\ddot{u}) = \xi \quad (7)$$

If the calculated value does not match the initially assumed damping ratio (ξ_0), the damping ratio is recalculated using Eq. (7), and the corresponding responses are updated accordingly. This procedure is repeated iteratively by adjusting the damping ratio until the free vibration equation is satisfied using a successive approximation method.

The analysis was performed for two cases: a constant damping ratio ($\xi = 0.05$) and a variable damping ratio defined by Eq. (7), both based on the general equilibrium equation (Eq. (8)). To ensure numerical consistency, the iterative process was continued until convergence was achieved, defined by a negligible difference between successive values of the damping ratio and the corresponding dynamic response. A convergence tolerance of 10^{-4} was adopted for the damping ratio variation between successive iterations.

After solving the general equation of motion, an Excel-based computational procedure was implemented to track all relevant variables, including the damping ratio at each time step and the associated dynamic responses (displacement, velocity, and acceleration), assuming an initial velocity value.

As a result, the variation of the damping ratio with time was obtained. In addition, a logarithmic representation of the damping ratio variation over a wide frequency range was generated by considering the reciprocal of the time step as an equivalent frequency. Fig. 3 illustrates the damping ratio variations obtained from the numerical analysis. The relationship between damping ratio and acceleration amplitude is described by Eqs. (9–10), as shown in Fig. 2.

The damping ratio variations in the time domain are presented in Fig. 3-a, while the variations in the frequency domain are shown in Fig. 3 (b–d).

$$m\,\ddot{u} + c\,\dot{u} + k u = 0 \quad (8)$$

$$\xi = 0.0305\,\ddot{u}^{\,0.2493} \quad (9)$$

$$m\,\ddot{u} + 2\omega m \times (0.0305\,\ddot{u}^{\,0.2493})\dot{u} + k u = 0 \quad (10)$$

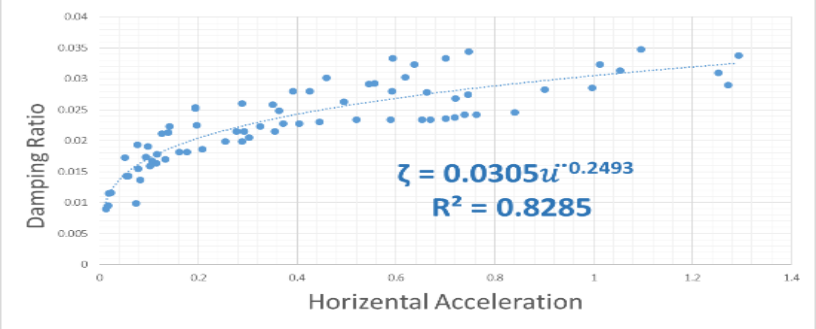

Fig (2) Damping ratio equation [15]

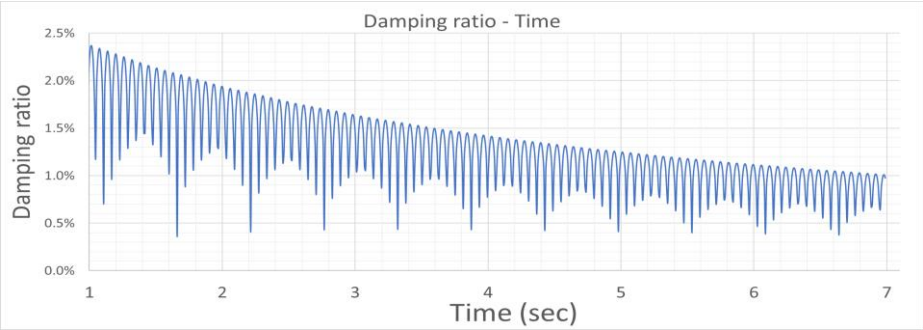

Fig (3.a) - Damping ratio – Time

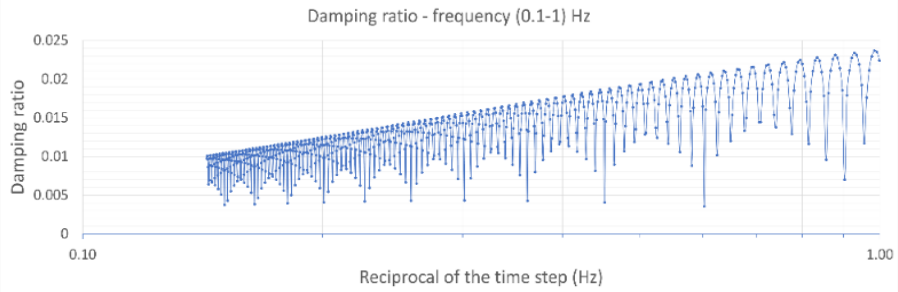

Fig (3. b) Damping ratio – frequency (0.1-1) Hz

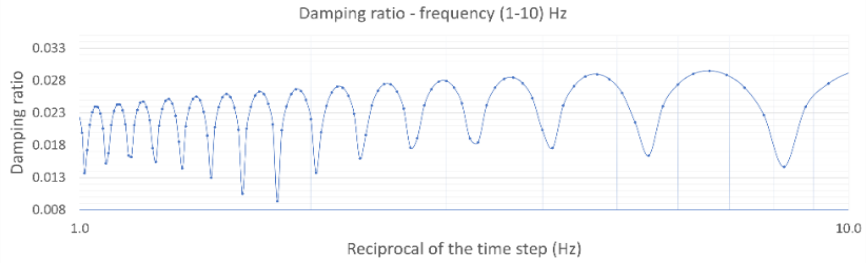

Fig (3.c) Damping ratio – frequency (1-10) Hz

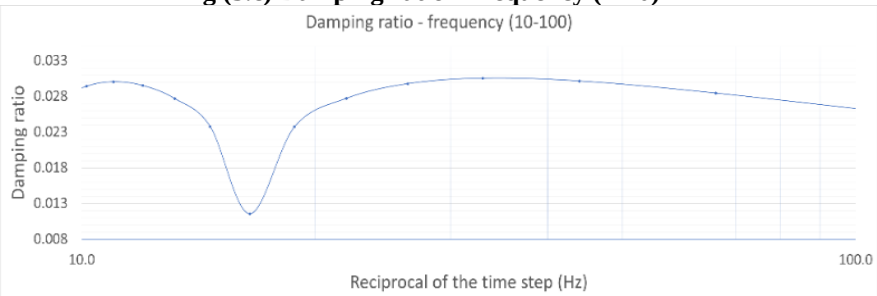

Fig (3.d) Damping ratio – frequency (10-100) Hz

Fig (3) Damping ratio variations in time and frequency domain

3- Analytical study:

1.3 Modeling description:

A numerical model simulating the experimental bridge specimens [16], shown in Fig. 4, was developed using the finite element software ABAQUS.

The model was discretized into finite elements of varying sizes, with mesh refinement adjusted according to the importance of each structural component, while considering computational efficiency and solution time.

A finer mesh was adopted for the slab, as it represents a critical component in accurately capturing the structural response. In the experimental setup, free vibration was induced by a hammer impact applied at the top of the bridge model, causing oscillation primarily about the weak axis of the cross-section.
The resulting horizontal acceleration responses were recorded using an accelerometer placed at the top of the model.To replicate the experimental conditions, an equivalent impulse load was applied in the numerical model to simulate the free vibration test. This modeling approach ensures consistency between the experimental setup and the numerical simulation, enabling reliable validation of the analytical results.

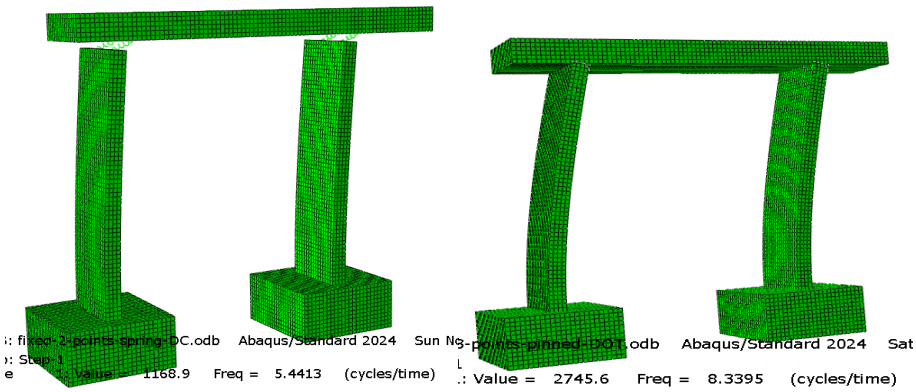

Fig (4.a)Abaqus model - Steel plate **Fig (4.b) Abaqus model – Rubber bearing**

Fig (4) Abaqus model of the RC bridge

3- Result discussion:

To validate the damping variation equation (Eq. (7)), the acceleration responses obtained from numerical and analytical analyses were compared with the experimental results. First, the natural frequencies of the first mode obtained from the numerical and analytical models for both fixed and LRB connections were compared with the corresponding experimental values. As shown in Table 1, a good agreement was observed, with only minor differences between the predicted and measured values. Subsequently, the acceleration time-history responses were evaluated considering both constant damping ($\xi = 5\%$) and variable damping ratio. Fig. 5 presents the comparison between numerical and experimental responses for the fixed slab–pier connection. It can be observed that, in the case of constant damping, the difference in peak acceleration reached approximately 50%, whereas the variable damping model significantly reduced this difference to about −2%. Similarly, Fig. 6 illustrates the comparison between analytical and experimental acceleration responses for both fixed and LRB connections.
For the fixed support case (Fig. 6-a), the difference in peak acceleration was about 58% for constant damping, while it decreased to approximately 1.5% when variable damping was considered. For the LRB case (Fig. 6-b), the difference was about 38% for constant damping and reduced to approximately 2.2% with variable damping. These results clearly indicate that the variable damping ratio provides a much closer agreement with the experimental response, particularly within the first 2 seconds of motion. In contrast, the constant damping assumption leads to significant discrepancies in the predicted response.
Furthermore, Fig. 7 compares the numerical, analytical, and experimental acceleration responses for the fixed connection case. The numerical results obtained using Excel show a strong agreement with the experimental data, with a difference of approximately 2% in peak acceleration. This confirms the validity of the proposed damping variation equation (Eq. (7)) and highlights the importance of incorporating damping variability in seismic response analysis. This improvement demonstrates the limitations of constant damping assumptions and emphasizes the necessity of adopting amplitude-dependent damping models for accurate seismic response prediction.
It is obvious that there was a significant convergence in the results up to 2sec for variable damping ratio, while it was large for constant damping ratio.

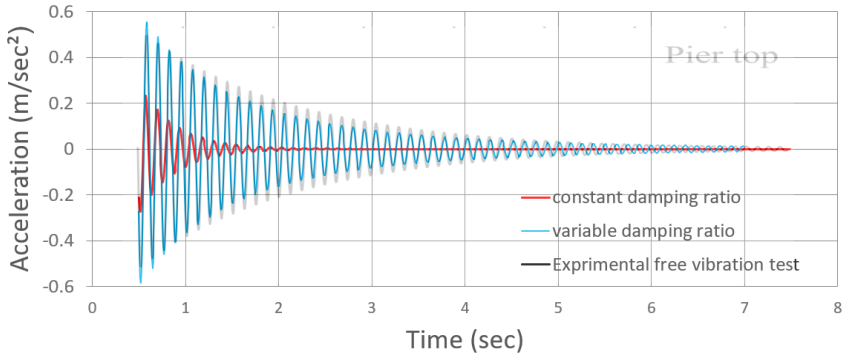

Fig (5) Numerical and experimental acceleration response of the RC bridge model(Fixed support)

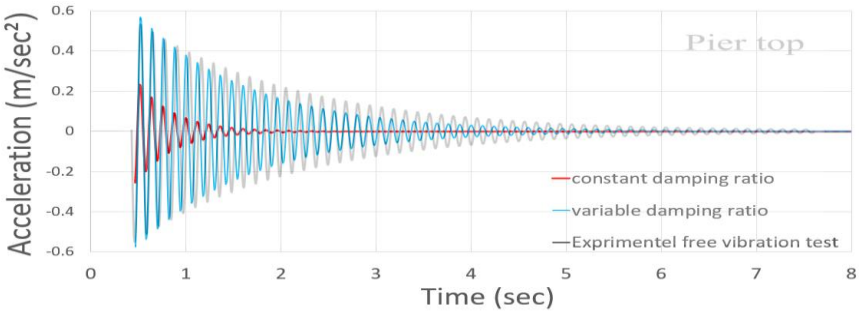

Fig (6-a) Fixed support

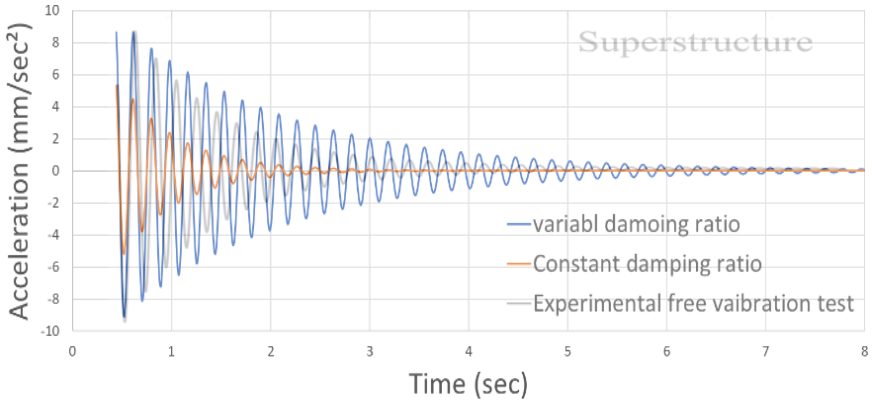

Fig (6-b) LRB support

Fig (6) Analytical and experimental acceleration response of the RC bridge model

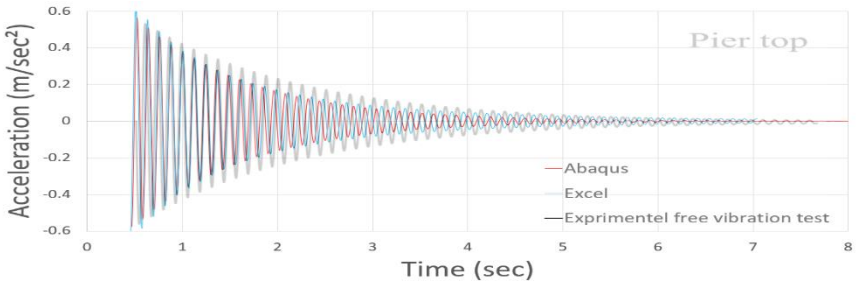

Fig (7) Numerical, analytical and experimental acceleration response (fixed support)

Table (1) Natural frequency

Bridge Model	Experimental	Excel	ABAQUS
F (Hz) – Steel plate	7.935	8.233	8.339
F (Hz) – Rubber Bearing	5.615	-	5.441

Furthermore, Fig. 7 presents a comparison between the numerical and analytical acceleration responses obtained using the variable damping ratio and the experimental acceleration response of the fixed-connection RC bridge model. It can be observed that the numerical results obtained using Excel show a significantly improved agreement with the experimental data, with a difference of approximately 2% in the maximum acceleration amplitude.

The comparison of the numerical, analytical, and experimental acceleration time-history responses in Fig. 7 confirms the validity of the adopted reference equation (Eq. (7)). When the variation of the damping ratio is taken into account, the predicted responses exhibit a closer agreement with the experimental results. This result further highlights the importance of incorporating damping ratio variability in accurately capturing the dynamic behavior of RC bridge systems. This result further highlights the importance of incorporating damping ratio variability in accurately capturing the dynamic behavior of RC bridge systems.

4- Seismic Response of the existing RC bridge:

a. Models' description:

After validating the proposed damping ratio variation equation, it was applied to an existing RC bridge, namely the Al-Houla Bridge (Fig. 8), located on the Homs–Houla road and constructed in 2006. The bridge consists of two spans of 18 m, supported by three piers and seven beams. The beam spacing is 140 cm, and the slab thickness is 20 cm, with cantilever extensions of 70 cm from the beam axis on each side.

Each pier consists of five columns, a cap beam, and bumpers at both abutments. The column cross-section is 70 × 70 cm with a reinforcement ratio of 1.5%. The column height is 6 m from ground level to the underside of the cap and 6.5 m to the beam axis. The cap beam has a thickness of 70 cm and a width of 100 cm. The bumper width is 70 cm with a net height of 120 cm. A clearance of 15 cm is provided between the bumper and the slab on each side to allow horizontal movement.

Neoprene supports were used to control the vibration of the bridge deck at both ends. Since the mechanical properties of these supports were not available, a series of laboratory tests was conducted at Homs University, including shear, axial compression, and rotation tests, to determine their mechanical characteristics for use in the numerical model.

The dimensions of the neoprene bearings are 200 × 200 × 46.81 mm. The thickness of the main neoprene layer is 7.19 mm, while the effective total thickness of the internal layers is 28.75 mm. The steel plate

thickness varies between 2 mm and 2.15 mm, with an average spacing of 2.07 mm, resulting in a total thickness of 10.35 mm.

Based on the experimental characterization, the equivalent stiffness values of the supports were determined as $k_{xx} = 4.41 \times 10^6$ N/m and $k_{zz} = 4.41 \times 10^6$ N/m for horizontal directions, and $k_{yy} = 1.64 \times 10^8$ N/m for the vertical direction. This detailed characterization ensures that the numerical model accurately represents the actual structural and support conditions of the bridge.

Fig (8). Al-Houla Bridge (a camera photo)

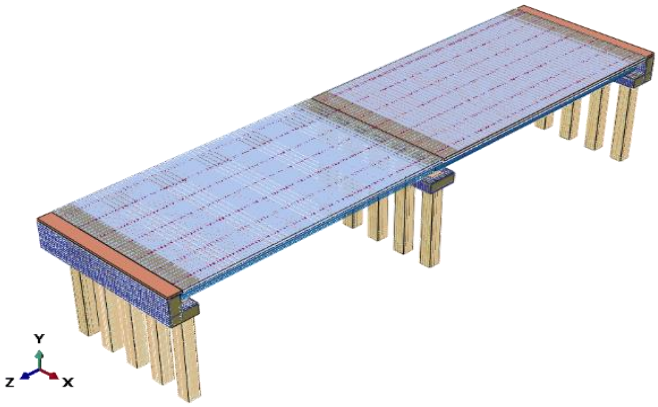

Fig (9) Abaqus model of Houla bridge

b. Modeling description:

In this study, the bridge was modeled using ABAQUS software. The supports of the bridge piers were assumed to be fixed at the foundation level, while the superstructure was modeled with appropriate boundary conditions restraining the required degrees of freedom. Neoprene supports were represented in the numerical model using equivalent horizontal and vertical spring elements. Concrete was modeled using solid homogeneous elements (C3D8), while reinforcement was represented using truss elements (T3D2). The lead rubber bearings were simulated using spring and dashpot elements (CO3D2). The nonlinear behavior of concrete in the plastic range was incorporated through an appropriate stress–strain relationship based on the fundamental material properties [15]. Fig. 10 illustrates the adopted stress–strain relationship for concrete. The adopted modeling approach ensures a realistic representation of both structural components and support conditions, enabling accurate simulation of the seismic response.

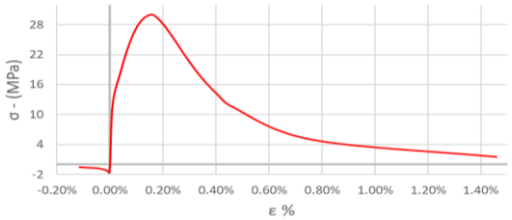

Fig (10) Concrete (Stress-Strain)

c. Seismic analysis response:

The seismic analysis of the RC bridge was performed using ABAQUS under two different damping assumptions. In the first case, a constant damping ratio of $\xi = 0.05$ was considered, while in the second case, a variable damping ratio was applied at each time step according to Eq. (9) [15], as illustrated in Fig. 2. Based on the numerical procedure developed in this study, the variation of the damping ratio was evaluated in both the time domain (Fig. 3-a) and the frequency domain (Fig. 3 (b–d)).

The seismic input was defined using the Turkey–Syria (Hatay) earthquake record (station TK 3123), associated with the seismic events of 6 February 2023 and subsequent aftershocks shown in Fig. 11 [19,20]. To investigate the influence of excitation intensity, different scaling factors of 30%, 50%, 70%, 100%, and 130% of the recorded ground motion were applied. The corresponding dynamic responses of the bridge, including base shear forces, accelerations, displacements, and velocities, were obtained and compared for both constant and variable damping ratio cases under each excitation level. This approach allows for a comprehensive assessment of the influence of damping ratio variability on the seismic response under different levels of ground motion intensity.

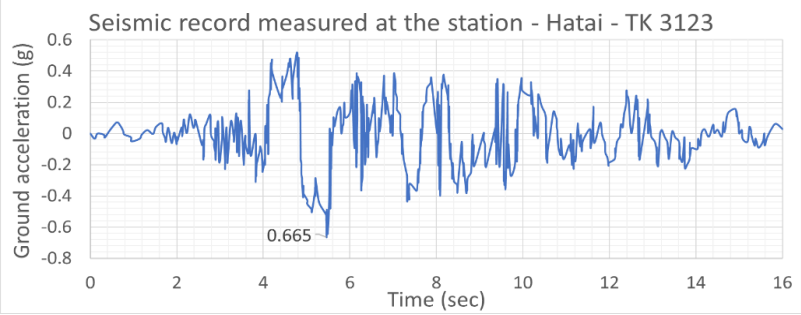

Fig (11) Turkey-Syria (Hatay – TK 3123) Record [20]

d. Result discussion:

Fig. 12 presents the time-history responses of the RC bridge (base shear, acceleration, displacement, and velocity) for both constant and variable damping ratios under 100% of the earthquake record. It can be observed that the responses obtained using the variable damping ratio are consistently higher than those obtained using the constant damping assumption. Furthermore, Fig. 13 illustrates the variation of the maximum responses for different scaling levels of the earthquake excitation.

It is evident that the maximum structural response increases with increasing excitation amplitude in both cases; however, the difference between the constant and variable damping responses becomes more pronounced at higher intensity levels.

For instance, at 30% excitation, the difference in maximum acceleration between the two cases is approximately 70.55 m/s², whereas it increases significantly to about 305.72 m/s² at 130% excitation. Similarly, the difference in base shear increases from 30.61 kN at 30% excitation to 132.62 kN at 130%.

The same trend is observed for velocity and displacement responses, where the differences increase from 1.80 m/s to 7.77 m/s and from 0.26 mm to 1.11 mm, respectively.

These results indicate that the influence of damping ratio variability becomes increasingly significant with higher seismic excitation levels. The use of a constant damping ratio may therefore lead to underestimation of seismic demand, particularly under strong ground motion conditions.

Overall, the incorporation of a variable damping ratio provides a more realistic representation of the seismic response of RC bridges, highlighting the importance of considering amplitude-dependent damping in practical seismic analysis and assessment.

This finding has important implications for seismic design and assessment, as neglecting damping variability may result in non-conservative estimations of structural response.

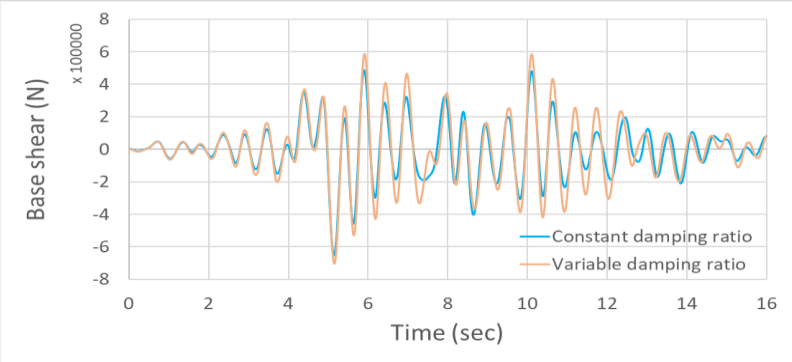

Fig (12.a) base shear force for Turkey 100% record

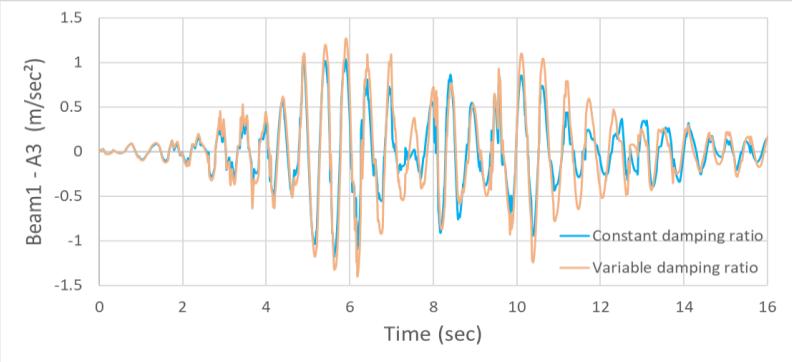

Fig (12.b) Superstructure acceleration response

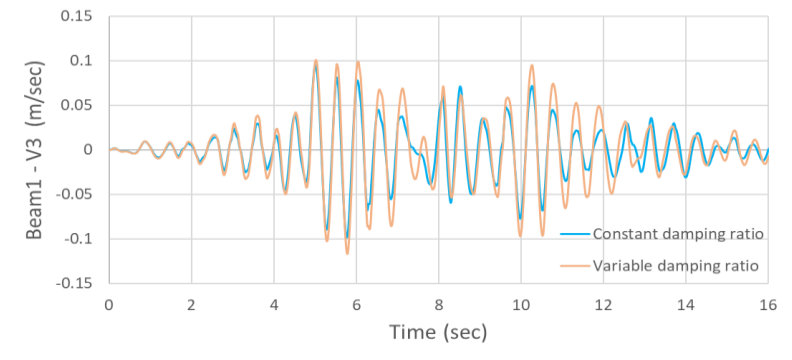

Fig (12.c) Superstructure velocity responses

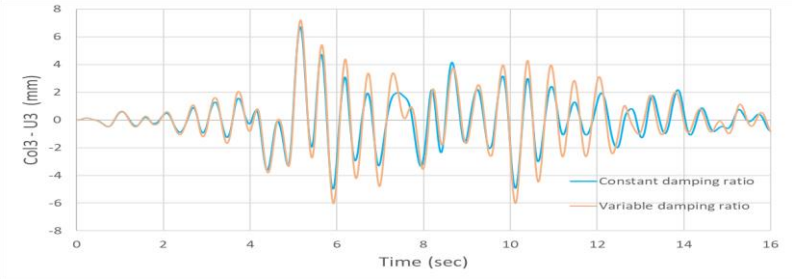

Fig(12.d) Middle column displacement response
Fig. 12 RC bridge seismic response

10 Conclusions and Recommendations:

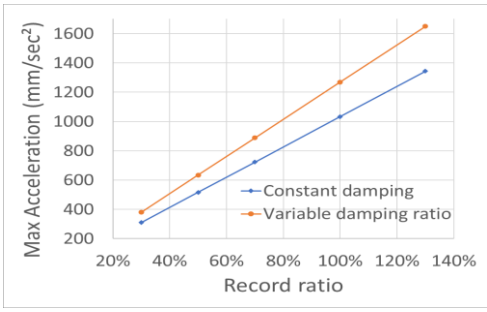

Fig (13-a) Beam Max acceleration responses

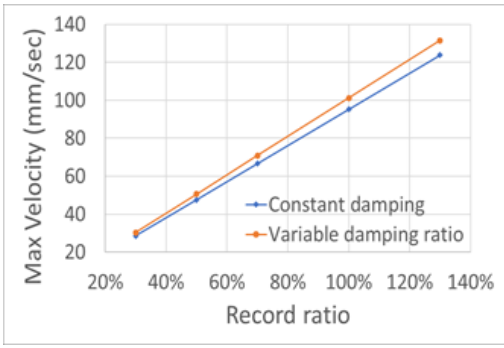

Fig (13. c.) Beam 1 Max velocity responses

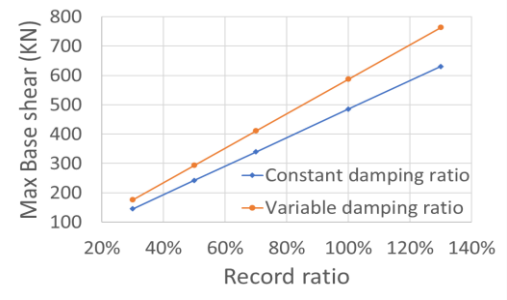

Fig (13-b) Max Base shear values from five records excitations

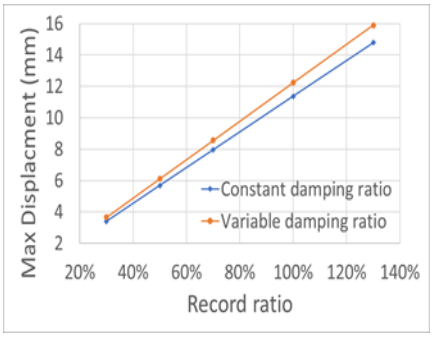

Fig(13-d) Beam 1 Max displacement responses

Fig (13) Maximum response for different excitation amplitude scaling

http://journal.damascusuniversity.edu.sy/index.php/index/index
X085-3031 :ISSN (online)

In this study, two analytical models simulating experimental single-span RC bridges were developed using ABAQUS software. The acceleration-dependent damping model proposed by Ghassoun et al. (2023) [15] was adopted to investigate the influence of damping ratio variation on seismic response. The proposed approach was first validated against experimental results and subsequently applied to an existing RC bridge. The main conclusions of this study can be summarized as follows:

1. The acceleration responses obtained from numerical and analytical analyses using the variable damping ratio showed very good agreement with experimental results, with differences ranging between 1.5% and 2.2%, compared to 38–58% for the constant damping ratio.
2. The proposed damping model resulted in higher seismic response estimates compared to the constant damping assumption. The base shear, displacement, acceleration, and velocity responses of the existing RC bridge increased when damping variability was considered.
3. The maximum seismic response of the bridge increased with increasing excitation amplitude, with a more pronounced difference between constant and variable damping cases at higher intensity levels.
4. The results demonstrate that assuming a constant damping ratio may lead to underestimation of seismic demand, whereas incorporating damping variability provides a more realistic representation of structural behavior under seismic loading.
5. In this study, numerical analysis was performed using Excel; however, for future work, it is recommended to develop a dedicated computational tool, such as a Python-based program, to efficiently implement the proposed damping model and facilitate its integration with finite element platforms such as ABAQUS.

Overall, the findings highlight the importance of considering amplitude-dependent damping in the seismic analysis and assessment of existing RC bridges.

Funding: This Research is funded by Damascus University-Funder no (501100020595).

References:

[1] Li, Ming, Wu. (2013). 1. Dynamic Response Analysis of Reinforced Concrete Suspension Bridge under Seismic Action. Applied Mechanics and Materials, doi: 10.4028/WWW.SCIENTIFIC.NET/AMM.405-408.

[2] Diego, Rodríguez, Martínez., Mervyn, J., Kowalsky. (2023). 1. Nonlinear seismic performance of RC bridges using the ESA, EDA, DDBA, and nonlinear analysis with various viscous damping models. Earthquake Spectra, doi: 10.1177/87552930221145435.

[3] Hafsa, Farooq. (2021). A comparative study of RC bridge for evaluation of seismic performance and retrofit technology. Innovative Infrastructure Solutions, doi: 10.1007/S41062-020-00424-6.

[4] Germán, Nanclares., Daniel, Ambrosini., Oscar, Curadelli., Martín, Domizio. (2020). 3. Nonlinear dynamic analysis of a RC bridge subjected to seismic loading. Smart Structures and Systems, doi: 10.12989/SSS.2020.26.6.765.

[5] Chin-Kuo, Su., Yu-Chi, Sung., Shuenn-Yih, Chang., Chao-Hsun, Huang. (2007). 4. Analytical Investigations of Seismic Responses for Reinforced Concrete Bridge Columns Subjected to Strong Near-fault Ground Motion. Earthquake Engineering and Engineering Vibration, doi: 10.1007/S11803-007-0757-8.

[6] Zhang, Jing. (2009). 5. Discussion on damping models for seismic response analysis of long-span bridge. Journal of Vibration and Shock.

[7] Adnan, Kıral., Ali, GÜRBÜZ., İlker, Ustabaş. (2024). 8. The Seismic Response Evaluation of an Existing Multi-span Reinforced Concrete Highway Bridge in the Presence of Linear and Nonlinear Viscous Dampers. Arabian journal for science and engineering, doi: 10.1007/s13369-024-09265-2.

[8] H. Shibata, (2001), "Project on 3-D Full-Scale Earthquake Testing Facility (the Second Report)," pp. 1–8, 2001.

[9] P. Paultre, O. Chaallal , J. Proulx (1992) "Bridge-dynamics-and-dynamic-amplification-factors-a-review-of-analytical-and-experimental-findings." Canadian Science Publishing Canadian Journal of Civil Engineering, April 199219(2):260-278, DOI:10.1139/l92-032.

[10] M. Celebi, (1999) "Radiation damping observed from seismic responses of buildings."12WCEE2000-2634.

[11] D. H. Lee, D. Kim, and T. Park, Jul. (2009) "Earthquake response analysis of RC bridges using simplified modeling approaches," J. Sound Vib., vol. 324, no. 3–5, pp. 640–665.

[12] Hall, J.F. (2006). Problems encountered from the use (or misuse) of Rayleigh damping. Earthquake Engineering & Structural Dynamics, 35(5), 525–545.

[13] Charney, F.A. (2008). Unintended consequences of modeling damping in structures. Journal of Structural Engineering, 134(4), 581–592.

[14] Priestley, M.J.N., Calvi, G.M., Kowalsky, M.J. (2007). Displacement-Based Seismic Design of Structures. IUSS Press.

[15] M. Ghassoun, R. ALsehnawi (2023) "Analytical prediction of damping coefficient-vibration amplitude Relationship changes of reinforced concrete bridge piers" Damascus university journal for the engineering sciences-No.9510.

[16] R. Alsehnawi, A. Nakajima, March (2016),"'Experimental Study on Dynamic Characteristic Dependency of Bridge Structures On Vibration Amplitude", a dissertation submitted to the faculty of engineering and the committee on graduate studies of graduate school of engineering, utsunomiya university in partial fulfillment of the requirements for the degree of doctor of philosophy in sustainable design and eng. Course.

[17] A. k. Chopra, (2012), Dynamics Of Structures Chopra 4d Ed.

[18] A. Belarbi, T. Hsu (1995) ,"Constitutive Laws of Softened Concrete in Biaxial Tension Compression _ Semantic Scholar." Engineering, Materials Science, Aci Structural Journal, DOI:10.14359/907Corpus ID: 138898242.

[19] Tetsuo, Tobita., Takashi, Kiyota., Seda, Torisu., O., Cinicioglu., Gokce, Tonuk., Nikolay, Milev., Juan,

Contreras., Othón, Contreras., Masataka, Shiga. (2024). 2. Geotechnical damage survey report on February 6, 2023 Turkey-Syria Earthquake, Turkey. Soils and Foundations, doi: 10.1016/j.sandf.2024.101463
[20] Seda, Yolsal-Çevikbilen., Tuncay, Taymaz., Tahir, Serkan, Irmak., Ceyhun, Erman., Metin, Kahraman., Berkan, Özkan., Tuna, Eken., Taylan, Öcalan., Ali, Hasan, Doğan., Cemali, Altuntaş. (2024). 3. Source Geometry and Rupture Characteristics of the 20 February 2023 Mw 6.4 Hatay (Türkiye) Earthquake at Southwest Edge of the East Anatolian Fault. Geochemistry Geophysics Geosystems, doi: 10.1029/2023gc011353